CHAPTER 4

CHARACTERIZATION OF IONIC LIQUIDS

4.1. Ionic liquid synthesis

The synthesis procedures of methylimidazole and triethylamine based cations with the alkyl-HSO_3^- chains and HSO_4^- as anion are published elsewhere [264, 265].

In some instances slight modifications were done to the established procedures. However, the alkyl-HSO_3 chain combination with butylimidazole, diethyl methylamine and both pyrazoles based cations, followed by combination with H_2SO_4 are new methods initially established in this research. The advantage of these ILs is that no byproduct will be produced during the synthesis. Hence, no addition chemicals are required for further purification.

4.2. Identification of ILs

Before conducting further characterization tests, the ILs were first proven by proton nuclear magnetic resonance analysis (^{1}HNMR) and CHNS elemental analysis.

Then their purity in terms of water content, viscosity, and density, and thermal behaviors in terms of melting and decomposition points were characterized. The results of each characterization test are presented and discussed in this chapter.

4.2.1. Colour by visual observation

There is a general agreement that 100% pure ILs should be colourless and halide free after being extensively purified [26]. Yet, even when the halide route synthesis was avoided and after extensive washing of the synthesized ILs, the ammonium and imidazolium still have the same yellowish colours; only pyrazolium ILs give clear colourless liquid as shown in Figure 4.1.

This yellowish colour might be due to the cation nature, indicating the effects of cations on ionic liquid colour, while such effect is not observed in anion based ionic liquids.

However, it should be noted that the understanding of the physical and chemical properties of ILs is still limited [266].

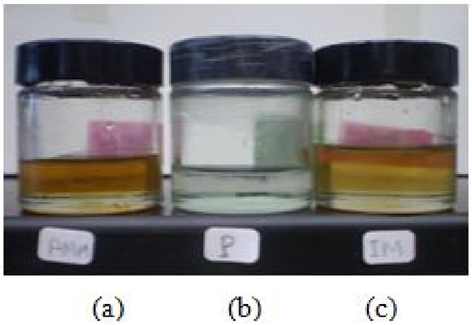

Figure 4.1 The colours of the functionalized SO_3H synthesized ILs (a) $DEMSBAMHSO_4$; (b) $SBPHSO_4$; and (c) $BSBIMHSO_4$.

4.2.2. NMR and CHNS analysis

The structures of the 24 compounds were confirmed by ^{1}HNMR using Bruker 300 MHZ NMR spectroscopy. Proton NMR spectra of the zwitterionic and RTILs were measured in DMSO.

Figure 4.2 presents the ^{1}HNMR spectrum and peaks identification for $BSPIMHSO_4$. The NMR results for other anion based ILs are detailed in Table 4.1. Examples of each cation were shown in Appendix B.

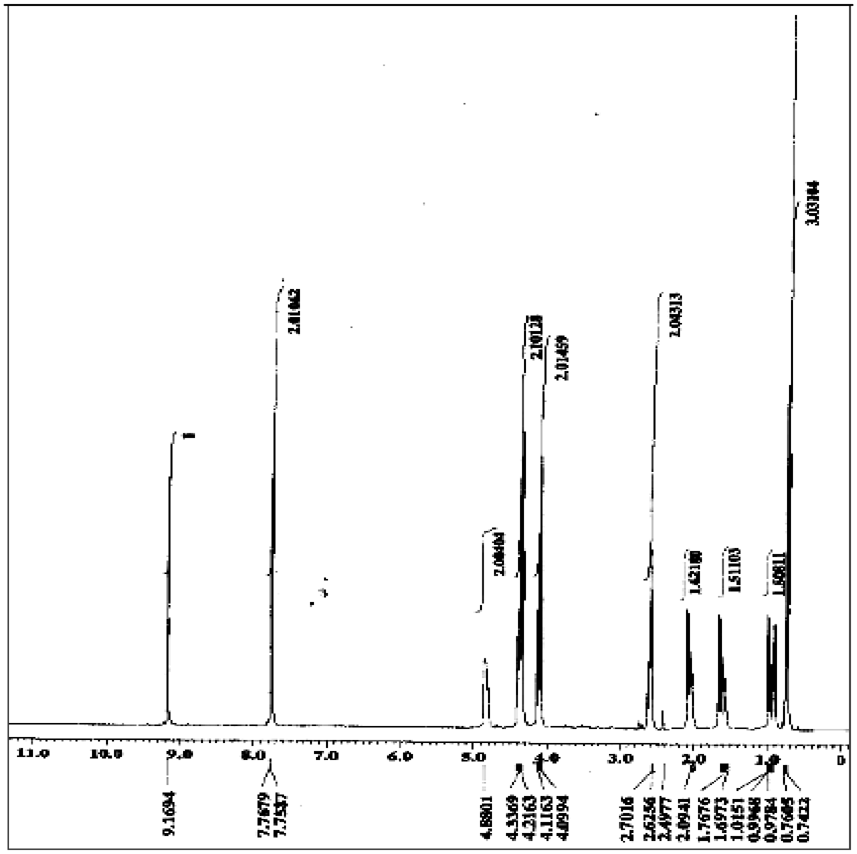

Figure 4.2 Proton NMR spectrum for BSPIMHSO$_4$. The peaks 1-11 indicated, $C\underline{H_3}$-C-, CH_3-$C\underline{H_2}$-, CH_3-C-$C\underline{H_2}$-, -N-C-$C\underline{H_2}$-C-S-, CH_3-C-C-$C\underline{H_2}$-, -S-$C\underline{H_2}$-, -N-$C\underline{H_2}$-C-C-S-, $O\underline{H}$, -N-$C\underline{H}$-C-N-,-N-C-$C\underline{H}$-N-, and -N-$C\underline{H}$-N-, respectively.

The molecular formula was determined from the CHNS results and molecular weights were calculated from the percentages obtained these data, shown in Appendix C. Also the yields of each IL are also calculated based on the weight percentages and listed in Table 4.1.

Table 4.1 Yields, ^{1}HNMR data and other properties of the synthesized ILs

Structure code	Molecular formula	Mwt (g/mol)	Yield (%)	1H NMR δ (300 MHz)
MPSIM	$C_7H_{12}N_2O_3S$	204.248	98.4	8.688 (s, 1H) 7.337 (s, 1H)

				7.198 (s, 1H) 4.183–4.232 (t, 2H) 3.712 (s, 3H) 2.706–2.753 (t, 2H) 1.975–2.184 (m, 2H)
MSPIMHSO$_4$	$C_7H_{14}N_2O_7S_2$	302.327	95.9	8.486 (s, 1H) 7.147 (s, 1H) 7.134 (s, 1H) 4.830 (s, 2H) 4.158–4.186 (t, 2H) 3.697 (s, 3H) 2.648–2.681 (t, 2H) 1.827–1.877 (m, 2H)
MBSIM	$C_8H_{14}N_2O_3S$	218.274	95.7	8.987 (s, 1H) 7.787 (s, 1H) 7.746 (s, 1H) 4.204–4.255 (t, 2H) 3.971 (s, 3H) 2.678–2.715 (t, 2H) 1.842 – 1.901 (m, 2H) 1.554–1.578 (m, 2H)

Table 4.1 Yields, ^{1}HNMR data and other properties of the synthesized ILs (continue)

Structure code	Molecular formula	Mwt (g/mol)	Yield (%)	1H NMR δ (300 MHz)
MSBIMHSO$_4$	$C_8H_{16}N_2O_7S_2$	316.354	95.4	9.182 (s, 1H) 7.782 (s, 1H) 7.723 (s, 1H) 5.007 (s, 2H) 4.177–4.158 (t, 2H) 3.860 (s, 3H)

				2.592–2.634 (t, 2H) 1.835–1.878 (m, 2H) 1.535–1.557 (m, 2H)
BPSIM	$C_{10}H_{18}N_2O_3S$	246.328	93.8	8.978 (s, 1H) 7.776 (s, 1H) 7.756 (s, 1H) 4.262–4.351 (t, 2H) 4.079–4.103 (t, 2H) 2.672–2.738 (t, 2H) 2.098–2.145 (m, 2H) 1.627–1.676 (m, 2H) 1.164–1.190 (m, 2H) 0.670–0.712 (t, 3H)
$BSPIMHSO_4$	$C_{10}H_{20}N_2O_7S_2$	344.407	95	9.169 (s, 1H) 7.768 (s, 1H) 7.759 (s, 1H) 4.880 (s, 2H) 4.216–4.337 (t, 2H) 4.099–4.116 (t, 2H) 2.626–2.713 (t, 2H) 2.094–2.121 (m, 2H) 1.697–1.768 (m, 2H) 0.978–1.015 (m, 2H) 0.742–0.761 (t, 3H)

Table 4.1 Yields, ^{1}HNMR data and other properties of the synthesized ILs (continue)

Structure code	Molecular formula	Mwt (g/mol)	Yield (%)	1H NMR δ (300 MHz)
BBSIM	$C_{11}H_{20}N_2O_3S$	260.354	92	9.169 (s, 1H) 7.719 (s, 1H) 7.656 (s, 1H) 4.223–4.335 (m, 2H) 4.021–4.050 (t, 2H) 2.467–2.501 (m, 2H) 1.804–1.888 (m, 2H) 1.609–1.641 (m, 2H)

				1.376–1.401 (m, 2H) 0.827–0.841 (t, 3H)
BSBIMHSO$_4$	$C_{11}H_{22}N_2O_7S_2$	358.434	94.9	9.156 (s, 1H) 7.775 (s, 1H) 7.704 (s, 1H) 4.975 (s, 2H) 4.131–4.167 (t, 2H) 3.969–3.997 (t, 2H) 2.897–2.913 (t, 2H) 2.346–2.420 (m, 2H) 1.759–1.777 (m, 2H) 1.548–1.580 (m, 2H) 1.198–1.240 (m, 2H) 0.814–0.823 (t, 3H)
PSP	$C_6H_{10}N_2O_3S$	190.221	89.4	7.914 (s, 1H) 7.852 (s, 1H) 6.496 (s, 1H) 4.797 (s, 1H) 4.379–4.461 (t, 2H) 2.742–2.796 (t, 2H) 2.118–2.188 (m, 2H)

Table 4.1 Yields, ^{1}HNMR data and other properties of the synthesized ILs (continue)

Structure code	Molecular formula	Mwt (g/mol)	Yield (%)	1H NMR δ (300 MHz)
SPPHSO$_4$	$C_6H_{12}N_2O_7S_2$	288.301	94.5	7.922 (s, 1H) 7.765 (s, 1H) 6.416 (s, 1H) 5.007 (s, 3H) 4.682 – 4.725 (t, 2H) 2.695 – 2.756 (t, 2H) 2.054 – 2.193 (m, 2H)
BSP	$C_7H_{12}N_2O_3S$	204.248	88.9	7.996 (s, 1H) 7.832 (s, 1H) 6.642 (s, 1H)

				5.227 (s, 1H) 4.224–4.268 (t, 2H) 2.857–2.903 (t, 2H) 2.196 – 2.265 (m, 2H) 1.881–1.932 (m, 2H)
SBPHSO$_4$	$C_7H_{14}N_2O_7S_2$	302.327	95	7.888 (s, 1H) 7.804 (s, 1H) 6.711 (s, 1H) 5.092 (s, 3H) 4.521–4.563 (t, 2H) 2.947–2.993 (t, 2H) 2.188–2.224 (m, 2H) 1.957–2.018 (m, 2H)
MPSP	$C_7H_{12}N_2O_3S$	204.248	89.1	8.108 (s, 1H) 7.928 (s, 1H) 6.513 (s, 1H) 4.423–4.462 (t, 2H) 3.932 (s, 3H) 2.888–2.901 (t, 2H) 1.885–2.049 (m, 2H)

Table 4.1 Yields, ^{1}HNMR data and other properties of the synthesized ILs (continue)

Structure code	Molecular formula	Mwt (g/mol)	Yield (%)	1H NMR δ (300 MHz)
MSPPHSO$_4$	$C_7H_{14}N_2O_7S_2$	302.327	91.9	8.012 (s, 1H) 7.860 (s, 1H) 6.459 (s, 1H) 4.888 (s, 2H) 4.338–4.345 (t, 2H) 3.913 (s, 1H) 2.800–2.853 (t, 2H) 2.078–2.174 (m, 2H)
MBSP	$C_8H_{14}N_2O_3S$	218.274	94.7	8.112 (s, 1H) 7.985 (s, 1H) 6.414 (s, 1H) 4.211–4.272 (t, 2H) 3.982 (s, 3H) 2.671–2.701 (t, 2H)

				1.877–1.911 (m, 2H) 1.561–1.658 (m, 2H)
MSBPHSO$_4$	$C_8H_{16}N_2O_7S_2$	316.354	90.5	8.117 (s, 1H) 7.991 (s, 1H) 6.423 (s, 1H) 4.797 (s, 1H) 4.202–4.268 (t, 2H) 3.977 (s, 3H) 2.666–2.693 (t, 2H) 1.874–1.906 (m, 2H) 1.557–1.650 (m, 2H)
DEMPSAM	$C_8H_{19}NO_3S$	209.307	90	3.196–3.535 (q, 2H) 3.016–3.058 (t, 2H) 2.809–2.946 (t, 2H) 2.709 (s, 3H) 1.898–1.958 (m, 2H) 1.040–1.198 (t, 6H)

Table 4.1 Yields, ^{1}HNMR data and other properties of the synthesized ILs (continue)

Structure code	Molecular formula	Mwt (g/mol)	Yield (%)	1H NMR δ (300 MHz)
DEMSPAMHSO$_4$	$C_8H_{21}NO_7S_2$	307.387	90.1	5.007 (s, 2H) 3.179–3.448 (q, 2H) 3.012–3.050 (t, 2H) 2.845 – 2.918 (t, 2H) 2.705 (s, 3H) 1.797 – 1.914 (m, 2H) 1.002 – 1.129 (t, 6H)
DEMBSAM	$C_9H_{21}NO_3S$	223.334	90.3	3.108 – 3.509 (q, 2H) 3.026 – 3.083 (t, 2H) 2.769 – 2.936 (t, 2H) 2.708 (s, 3H) 1.716 – 1.942 (m, 4H) 1.081 – 1.198 (t, 6H)

DEMSBAMHSO$_4$	$C_9H_{23}NO_7S_2$	321.413	90.7	5.027 (s, 2H) 3.101 – 3.501 (q, 2H) 3.017 – 3.071 (t, 2H) 2.766 – 2.922 (t, 2H) 2.681 (s, 3H) 1.682 – 1.931 (m, 4H) 1.057 – 1.187 (t, 6H)
TEPSAM	$C_9H_{21}NO_3S$	223.334	82.5	3.308 – 3.409 (t, 2H) 3.026 – 3.063 (t, 2H) 2.763 – 2.800 (t, 4H) 1.692 – 1.749 (m, 2H) 1.031 – 1.102 (t, 6H)

Table 4.1 Yields, ^{1}HNMR data and other properties of the synthesized ILs (continue)

Structure code	Molecular formula	Mwt (g/mol)	Yield (%)	1H NMR δ (300 MHz)
TESPAMHSO$_4$	$C_9H_{23}NO_7S_2$	321.413	80.8	4.606 (s, 2H) 3.450–3.505 (t, 2H) 3.000–3.046 (t, 2H) 2.737–2.789 (t, 2H) 1.600–1.773 (m, 2H) 1.023–1.114 (t, 9H)
TEBSAM	$C_{10}H_{23}NO_3S$	237.361	83.6	3.123 – 3.189 (q, 2H) 3.032 – 3.097 (t, 2H) 2.765 – 2.802 (t, 2H) 1.823 – 1.919 (m, 4H) 1.046 – 1.108 (t, 6H)
TESBAMHSO$_4$	$C_{10}H_{25}NO_7S_2$	335.440	84	5.002 (s, 2H) 3.089 – 3.129 (q, 2H) 3.016 – 3.060 (t, 2H) 2.740 – 2.800 (t, 2H) 1.828 – 1.931 (m, 4H)

				1.44 – 1.187 (t, 6H)

4.3. Melting point

In order to discuss the melting point (m.p.) results, the ionic liquids are classified according to the anions, i.e., straight chain sulfonate anions and hydrogensulfate anion, and the alkyl chains.

According to the literature, ILs melting point increased as the length of the side chain is increased. This because increasing the alkyl chain giving stronger inter-molecular van der Waals forces, which give rise to greater melting points of chains. This trend also is explained in terms of cation - anion interactions in ionic liquids, such as van der Waals forces, hydrogen bonding and electrostatic forces [15, 267]. As can be seen in Table 4.2, the melting point decreases as the sulfonate side chain was increased from C3 to C4, while the same alkyl chain is kept constant on the other nitrogen. In the case of 1-alkyl-3-alkylsulfonate imidazolium ionic liquids, the melting point decreased from 122.5 °C for 1-methyl-3-propylsulfonate imidazolium (MSPIM), to 109 °C for 1-methyl-3-butylsulfonate imidazolium (MBSIM). Similarly, when the butyl chain replaced the methyl chain, the melting point dropped from 110 °C for 1-butyl-3-propylsulfonate imidazolium (BPSIM), to 40 °C for 1-butyl-3-butylsulfonate imidazolium (BBSIM). This observation may be associated with a possible destabilization of the crystalline state. Figure 4.3 shows DSC traces of the $BSBIMHSO_4$. It is observed that the IL shows a behavior of RTIL and have melting point of 5 °C for the second test run.

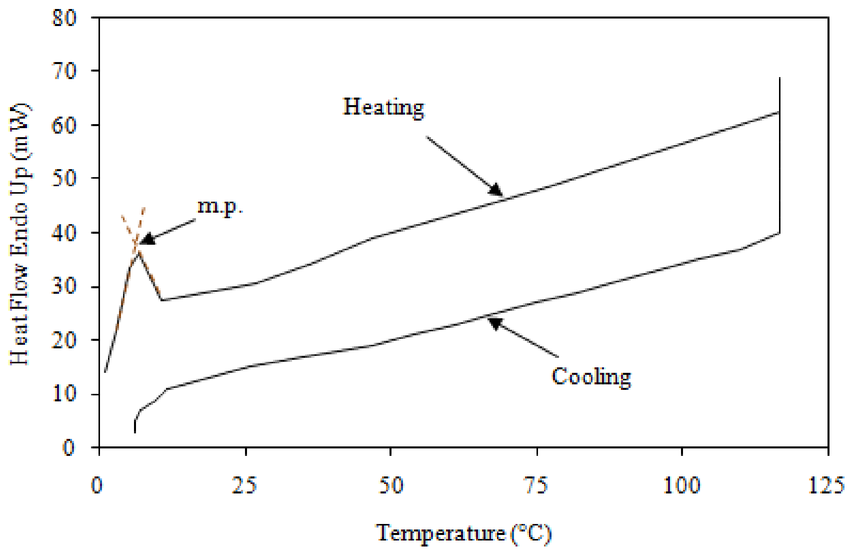

Figure 4.3 Differential scanning calorimetry result for $BSBIMHSO_4$.

For the corresponding zwitterionic ILs, 1-methyl-3-propylsulfonate imidazolium (MPSIM) and 1-methyl-2-propylsulfonate pyrazolium (MPSP), having the same molecular formula and molecular weight, however, they showed melting temperatures at 122.5 °C and 86.5 °C, respectively. Similarly, when combined with H_2SO_4, $MSPIMHSO_4$ showed higher melting of 10.5 °C compared with 1.5 °C with $MSPPHSO_4$. Accordingly, the pyrazoliums showed lower melting point than the imidazoliums ILs. These results are in contrast to the results described by Dunstan *et al*. [267], when they concluded that the dialkylimidazolium tetrafluoroborate had lower melting point than dialkylpyrazolium tetrafluoroborate. The ammonium ILs exhibit higher melting temperatures than the others as presented in Table 4.2.

Table 4.2 Melting points of imidazolium, pyrazolium and ammonium ILs

Structure code	m.p. (°C)
MPSIM	122.5 ± 1.2
MBSIM	109 ± 1
BPSIM	110 ± 1.2
BBSIM	40 ± 1.4
PSP	98.5 ± 0.9
BSP	54.5 ± 0.7
MPSP	86.5 ± 1.8
MBSP	74.5 ± 1.0
DEMPSAM	127 ± 0.7

DEMBSAM	122 ± 1.3
TEPSAM	134.5 ± 1.5
TEBSAM	154 ± 1.6
MSPIMHSO$_4$	10.5 ± 1.2
MSBIMHSO$_4$	8 ± 1.0
BSPIMHSO$_4$	6.5 ± 0.5
BSBIMHSO$_4$	4 ± 0.5
SPPHSO$_4$	3 ± 0.5
SBPHSO$_4$	- 1.5 ± 0.3
MSPPHSO$_4$	1.5 ± 0.4
MSBPHSO$_4$	-2.5 ± 0.6
DEMSPAMHSO$_4$	13 ± 1.4
DEMSBAMHSO$_4$	18.5 ± 1.5
TESPAMHSO$_4$	19.5 ± 1.5
TESBAMHSO$_4$	21 ± 1.1

Different from imidazolium and pyrazolium ILs, ammonium ILs show increasing melting point as the length of the side chain is increased, if it is alkyl or sulfonate chain. This indicates that the melting point is ruled by the side chain. These results are in agreement with Domańska [268] in his analysis for melting point of the C4 and C2 chains linked with ammonium cation with Br$^-$ as anion. In general, ammonium ILs show higher melting point than imidazolium and pyrazolium based cations.

4.4. Decomposition of ILs

The number of articles on synthesizing the ILs is increasing. However, there is still lack of data on their properties, which made the comparison with the literature difficult. This is because new ILs are being continuously designed.

Studies on thermal decomposition (T_{dec}) and effects of cation and side chain thermal behavior were carried out on all ILs. According to the literature, increasing the side chain of the cation decreases the thermal stability. The lowering of decomposition temperature could be due either to decrease of intermolecular interaction or to initial decomposition of the alkyl substituent [257, 268]. But there are exceptions described by many researchers. As well here in this research, increasing the side chain decreased the stability but also there are exceptions.

All of the synthesized salts exhibited good thermal stability and demonstrated high temperature of decomposition ranging from 280 ºC, as a lowest T_{dec} found for $TESBAMHSO_4$, to 372.8 ºC, as a highest T_{dec} found for BSPIM (see Appendix D). Changing the cation; from imidazolium, pyrazolium and ammonium with the same sulfonic side chain, i.e., propyl or butyl; produced different T_{dec}. Imidazolium and pyrazolium showed higher stabilities compared to the ammonium based ILs. The zwitterionic ILs with alkyl sulfonic functional group as anions showed higher thermal stabilities compared to the RTILs with alkyl sulfonic group side chain and HSO_4^- as anion. Nevertheless, the intermediate zwitterionic ammonium IL of DEMSPAM showed lower T_{dec} of 328 ºC, compared to 332.7 ºC of $DEMSPAMHSO_4$, after combining with H_2SO_4.

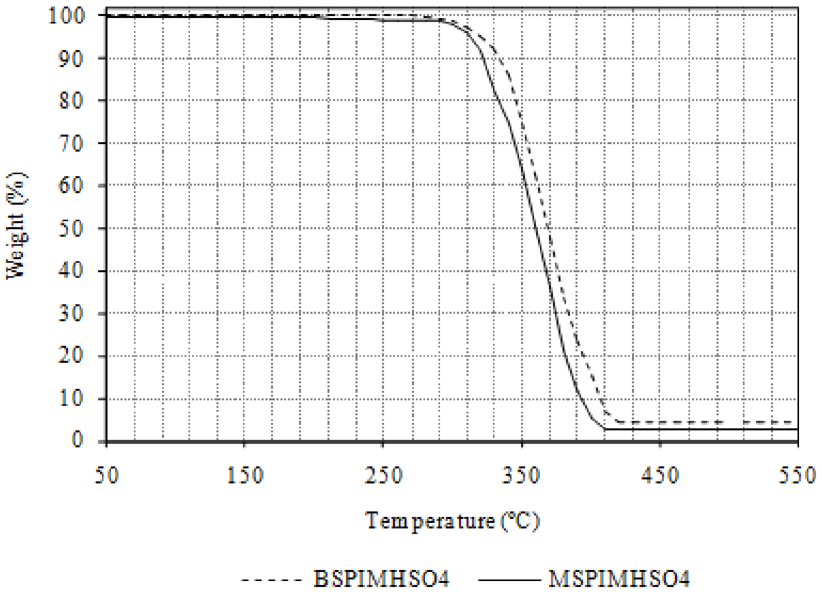

(a)

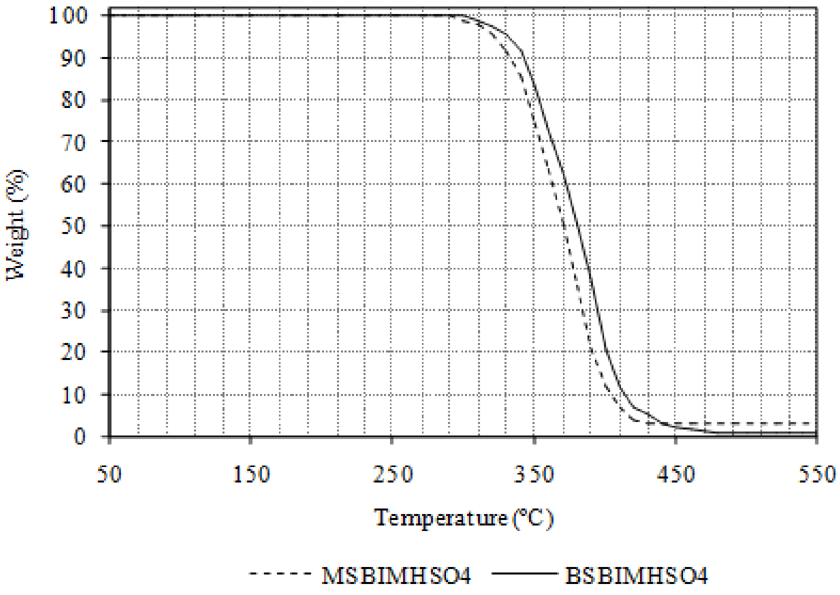

(b)

Figure 4.4 Thermogravimetric analysis (TGA) curves of the thermal decomposition of imidazolium ILs: (a) MSPIMHSO$_4$ and BSPIMHSO$_4$; (b) MSBIMHSO$_4$ and BSBIMHSO$_4$.

Studies on the effects of alkyl chain length and the alkyl sulfonic group side chain on T_{dec} showed that in imidazolium salts; for the shortest alkyl chain, i.e. CH_3 and propyl sulfonic chain in the cation, the T_{dec} equals to 315 ºC. Increasing the sulfonic chain from propyl to butyl decreases the T_{dec} to 306 ºC.

Changing the alkyl chain from CH_3 to C_4H_9, with propyl sulfonic chain, showed increasing thermal decomposition from 315 ºC to 323 ºC. On the other hand, varying the sulfonic chain from propyl to butyl decreases the T_{dec} to 306 ºC and 311.5 ºC for $MSBIMHSO_4$ and $BSBIMHSO_4$, respectively. In general, the rate of mass loss of imidazolium salts decreases with increasing alkyl chain length from methyl to butyl. Contradictory, the mass loss of imidazolium ILs increases with increasing functional alkyl chain length from propyl to butyl. Figures 4.4a and b show T_{dec} traces of the four imidazolium salts.

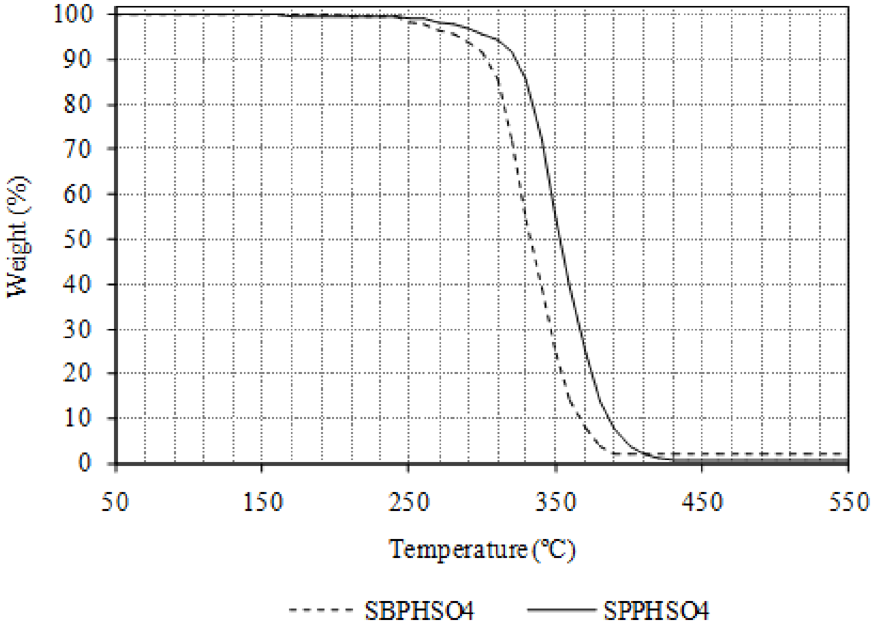

Figure 4.5 Thermogravimetric analysis (TGA) curves of the thermal decomposition of $SPPHSO_4$ and $SBPHSO_4$ pyrazolium ILs.

It can be seen that $MSPIMHSO_4$ compound starts to lose weight at ca. 250 ºC, while the IL $BSPIMHSO_4$ at 200 ºC. The TGA curves show that their thermal decomposition temperatures are almost the same, 315 and 323 ºC, respectively.

Varying the sulfonic chain from propyl to butyl, increases the weight loses, and making $MSBIMHSO_4$ and $BSBIMHSO_4$ less stable. $MSBIMHSO_4$ and $BSBIMHSO_4$ started to decompose at lower temperatures, ca. 270 ºC and 240 ºC, respectively.

For pyrazolium salts increasing the sulfonic chain linked with 1H-pyrazolium or 1-methyl-1H-pyrazolium from propyl to butyl showed vary small, almost unnoticeable increase in the T_{dec}. In general, as shown in Appendix D.1, the methyl pyrazolium salts has higher thermal stability than the pyrazolium salts.

Both pyrazolium and imidazolium exhibit similar behaviours. Their thermal decomposition occurred over a wide temperature range and their maximum rate of weight loss is almost the same.

As observed in Figure 4.5, these salts are stable up to 190 ºC and start to lose weight very slowly. For ammonium salts; their decomposition behaviour is different from imidazolium ones. It is noted that the percentage of mass loss of ammonium salts is higher than the other studied cations as indicated in Figures 4.6a and b; the decomposition started very late and finished very quickly. For instance, $TESPAMHSO_4$ started to lose the weight at 260 ºC, and completely decomposed at 295.4 ºC. This is perhaps due to that the ammonium is ruled by one nitrogen atom.

The zwitterionic ILs of diethyl methylamine of DEMSPAM and DEMSBAM showed lower stability than $DEMSPAMHSO_4$ and $DEMSBAMHSO_4$ after combining with H_2SO_4. This behaviour is different from the other ILs, even with triethylamine based cation.

The corresponding T_{dec} of ILs related to triethylamine based cation of IL TESPAM and $TESPAMHSO_4$ are almost the same, as well as the T_{dec} of TESBAM and $TESBAMHSO_4$. Increasing the chain length of alkyl or sulfonic side chain decreases the thermal stability. However as shown in Figures 4.6a and b, increasing the alkyl side chain from methyl to ethyl has greater effects on decreasing the T_{dec} than increasing the sulfonic chain.

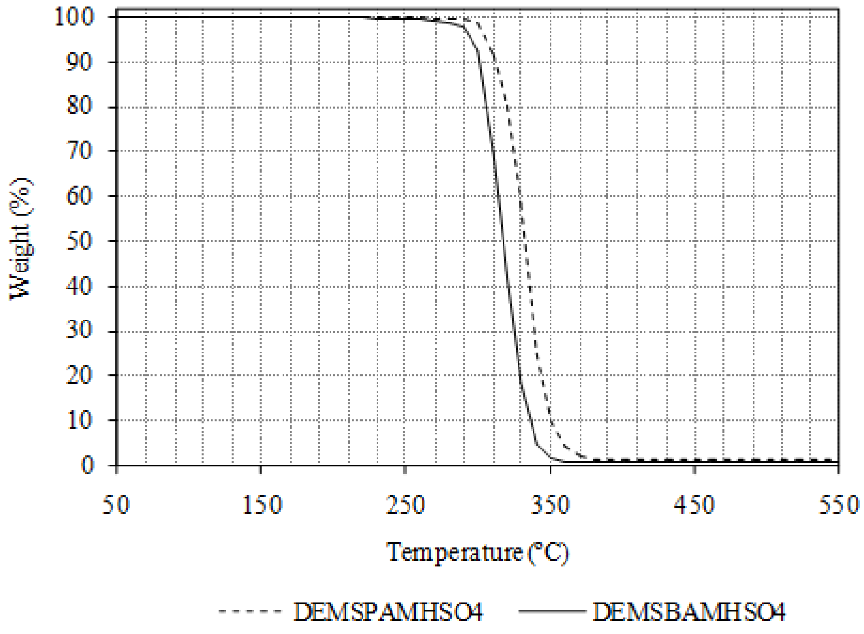

(a)

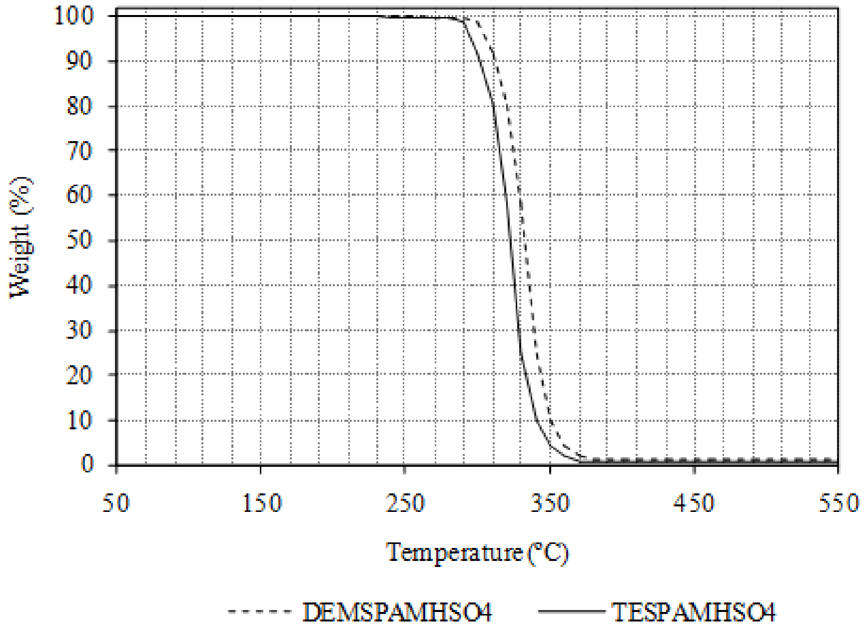

(b)

Figure 4.6 TGA traces for ammonium ILs: (a) $DEMSPAMHSO_4$ and $DEMSBAMHSO_4$; (b) $DEMSPAMHSO_4$ and $TESPAMHSO_4$.

4.5. Viscosity analysis

The viscosities for the ILs were analyzed as a function of temperature. Their measurements were obtained using an SVM 3000 Anton Paar. The analyses were performed in triplicate, in a temperature range of 20 to 80 °C. The absolute viscosity of ILs is usually reported in centipoises (cP) [26]. In order to discuss the effect of changing the side chain and the temperature on the ILs viscosities, the analyses were divided into three cation routes.

From engineering point of view, the viscosity of ILs is of prime importance as it is playing a major role in stirring and mixing. In addition, it affects one of the transport properties such as diffusion [32].

4.5.1. Imidazolium based cation

At 20 °C, the ILs MSPIMHSO_4, MSBIMHSO_4, BSPIMHSO_4 and BSBIMHSO_4 showed absolute viscosities of 1296, 1427, 1000, 1592 cP, respectively. Most of the obtained values are out the range of reported viscosity by other researches of being varied between 66 – 1110 cP [26, 32].

For the investigated imidazolium ILs, except for BSPIMHSO_4, the increase in one or both side chain length, either a sulfonate or an alkyl chain, on the cation will cause an increase in the viscosity. When the propylsulfonate chain, in MSPIMHSO_4, was replaced with butylsulfonate chain, in MSBIMHSO_4, a significant viscosity increase was observed from 1296 to 1427 cP, respectively. Similarly, changing the propylsulfonate in BSPIMHSO_4 to butylsulfonate in BSBIMHSO_4 increased the viscosity from 1000 to 1592 cP, respectively. When the methyl chain of MSBIMHSO_4 was changed to butyl chain giving BSBIM$HSO_{4,}$ the absolute viscosity increased from 1427 to 1592 cP. However, replacing the methyl chain in MSPIMHSO_4, with butyl chain, in BSPIMHSO_4, a considerable decrease in the viscosity was observed, from 1296 to 1000 cP, respectively. BSPIMHSO_4 showed a different viscosity behavior compared to others.

This unconformity indicates that the viscosity behaviour of ILs does not follow one rule. However, for the sulfonate side chain consistent viscosity behaviour was observed. This led to the conclusion that an increase in the sulfonate side chain length has a great effect on increasing the viscosity as it increased with increasing the sulfonate chain.

As can be seen in the Figure 4.7, the influence of temperature on viscosity is much more important than on density. In fact increasing the temperature leads to a reduced probability of the colliding molecules capturing one another. This strong decrease with increasing temperature makes the application of ILs in catalysis is easier at super-ambient conditions. However, no considerable decreased was observed over 60 °C [26].

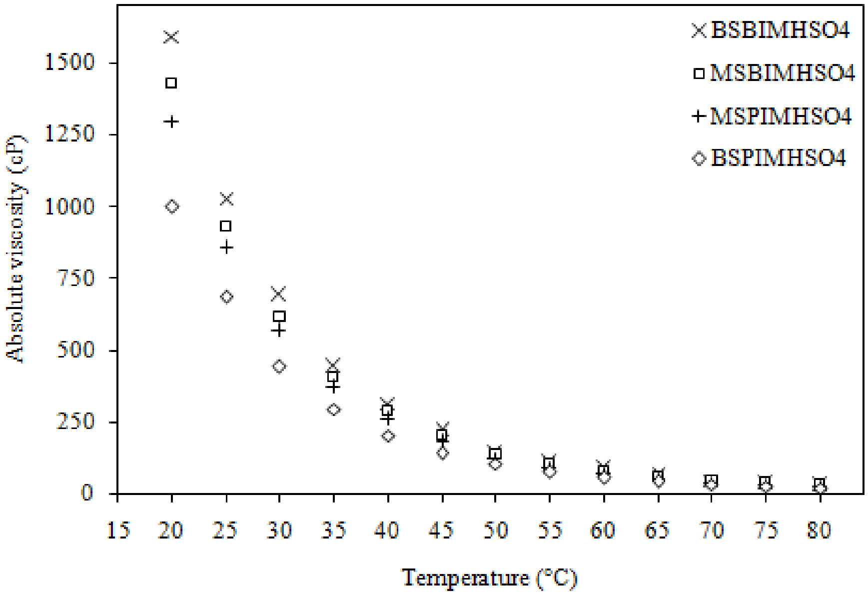

Figure 4.7 Viscosities of functionalized imidazolium ILs vs. temperature.

As noted, the ILs viscosities are strongly dependently upon temperature [26]. For example, as shown in Figure 4.7, the viscosity of $BSBIMHSO_4$ decreased about 91 %, with a 10 degree changes between 20 and 50 °C. Further increase in the temperature to 80 °C caused a decrease in the viscosity to 29 cP (98%). Other ILs too, showed decreasing viscosity with increasing temperature, as shown in Figures 4.8 and 4.9.

4.5.2. Ammonium based cation

Viscosities of the four ammonium based cation ILs were measured and the results are presented in Figure 4.8. Considerable viscosities increased were observed when the chain length of either one or both alkyl chains on the cation was increased. For example, at 20 °C, changing the methyl chain of $DEMSPAMHSO_4$ to ethyl, as in $TESPAMHSO_4$, increased the viscosity from 1062.4 to 1159.7 cP. Increasing the sulfonate chain of $DEMSPAMHSO_4$ from propyl to butyl, as $DEMSBAMHSO_4$, increased the viscosity from 1062.4 to 1664 cP. Increasing the length of sulfonate chain led to a significant increase in the viscosity compared to the alkyl chain. These results reveal that sulfonated chain has a greater effect on the salt viscosity than the alkyl chain.

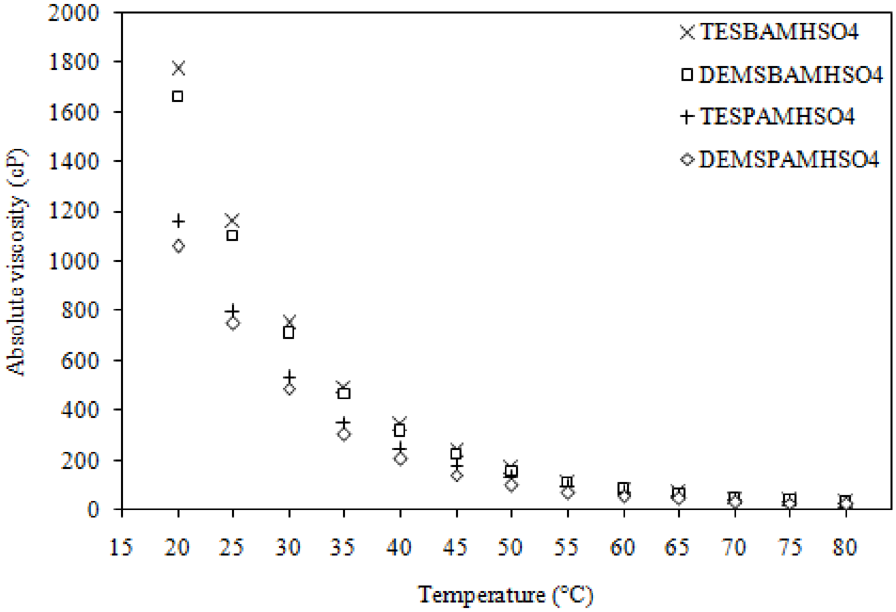

Figure 4.8 Viscosities of functionalized ammonium ILs vs. temperature.

4.5.3. Pyrazolium based cation

Generally, increasing length of an alkyl chain in a cation or anion increases the viscosity. However, there are exceptions presented in the literature. As well, for functionalized pyrazolium based cation, increasing the side chain increases the viscosity of the ILs, however, surprisingly, the viscosity increased in the order of $SPPHSO_4$> $MSBPHSO_4$> $SBPHSO_4$> $MSPPHSO_4$, as presented in Figure 4.9.

The obtained data show that the $SPPHSO_4$ has the highest viscosity with pyrazolium functional group attaining a viscosity of 1831 cP. When the propylsulfonate chain was replaced with butylsulfonate chain, the viscosity dropped from 1831 to 1762 cP. This result is in contrast with that of imidazoliums and ammoniums ones. On the other hand when the sulfonate chain was changed from propyl, in the $MSPPHSO_4$, to butyl, in $MSBPHSO_4$, the viscosity increased. These contradicting observations made it difficult to state one statute that can be tracked.

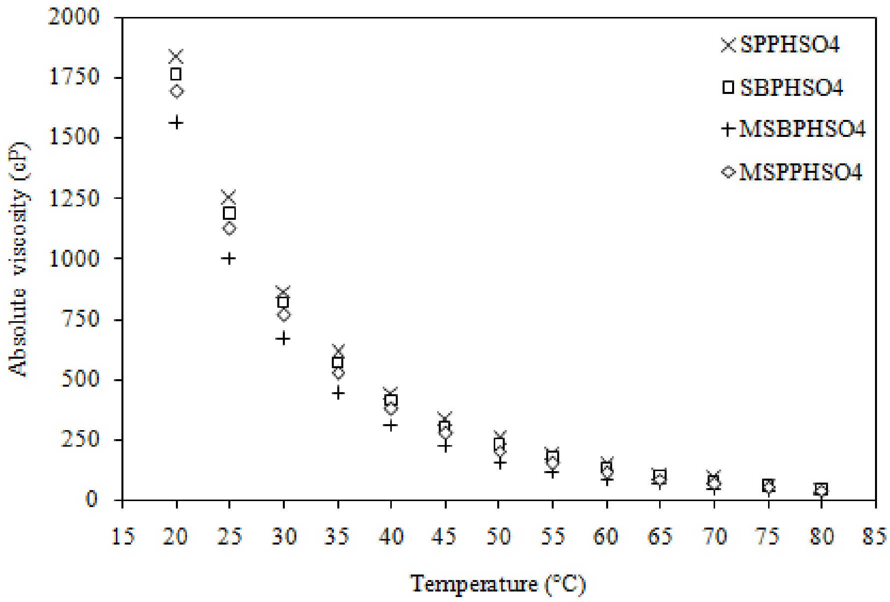

Figure 4.9 Viscosity of functionalized pyrazolium ILs vs. temperature.

As noted above, the pyrazoliums showed a trend of decreasing viscosity with increasing temperature, where MSBPHSO$_4$ measured a viscosity of 1558 cP at 20 °C. When the temperature was increased from 20 to 80 °C, the viscosity dropped significantly to 30.5 cP, a decrease of 98 %. However, the pyrazoliums did not show the same behavior of decreasing viscosities with increasing temperature, as the imidazolium ones.

Compared to others, the pyrazolium based ILs was found to be having higher viscosity. This may be attributed to the *N,N*'- ringed pyrazolium cations having a disk-like shape, which is predicted to favor the plastic behaviour [269].

4.6. Density analysis

The densities of the 12 ILs were measured at 20 °C and the results are presented in Table 4.3. As can be seen from the table, the densities varied from 1.35 to 1.58 g/cm^3. These results were in agreement with Valderrama and Zarricueta [270] who predicted that the ILs densities varied between 0.9 – 1.7 g/cm^3.

For the same cation, there are some changes in the density associated with changing the side chains. Several researchers have agreed the decrease of the density with increasing the temperature. And according to the literature, the density generally decreases with increasing length of an alkyl chain in a cation or anion.

For the same cation, there are some changes in the density associated with changes in the side chains. For example, when the methyl side chain in $MSPIMHSO_4$ was replaced by butyl side chain as in $BSPIMHSO_4$, the density dropped from 1.5048 to 1.3504 g/cm^3, respectively. Similarly the viscosity dropped when the methyl chain in $MSBIMHSO_4$, was replaced with butyl chain as in $BSBIMHSO_4$. The density dropped from 1.5048 to 1.4678 g/cm^3 when the propylsulfonate chain in $MSPIMHSO_4$ was replaced with butylsulfonate chain, as in $MSBIMHSO_4$. However, the density increased from 1.3504 to 1.3642 g/cm^3 when the propylsulfonate chain in $BSPIMHSO_4$ was replaced by butylsulfonate chain, as in $BSBIMHSO_4$. These results indicate that those ILs are not following one systematic behavior.

For the functionalized pyrazoliums, when the propylsulfonate of $SPPHSO_4$ was changed to butylsulfonate of $SBPHSO_4$, the density was reduced to 1.4443 g/cm^3. Nevertheless, replacing the propylsulfonate in $MSPPHSO_4$ with butylsulfonate of $MSBPHSO_4$ increased the density from 1.4183 to 1.4964 g/cm^3, respectively.

Table 4.3 Density data for imidazolium, pyrazolium and ammonium ILs (at 20 °C)

Structure code	Density (ρ), g/cm^3
$MSPIMHSO_4$	1.5048 ± 0.0003
$MSBIMHSO_4$	1.4678 ± 0.0001
$BSPIMHSO_4$	1.3504 ± 0.0005
$BSBIMHSO_4$	1.3642 ± 0.0003
$SPPHSO_4$	1.5253 ± 0.00009
$SBPHSO_4$	1.4443 ± 0.0002
$MSPPHSO_4$	1.4183 ± 0.00029
$MSBPHSO_4$	1.4964 ± 0.0004
$DEMSPAMHSO_4$	1.4731 ± 0.0005
$DEMSBAMHSO_4$	1.4532 ± 0.00038
$TESPAMHSO_4$	1.5814 ± 0.0004
$TESBAMHSO_4$	1.3642 ± 0.00045

The ammoniums also showed different behaviors like the others. For instance, decreasing the sulfonate chain, from butyl to propyl, showed increasing densities. Likewise, decreasing one of the alkyl chains, from ethyl of $TESBAMHSO_4$ to methyl of $DEMSBAMHSO_4$, showed increasing density from 1.3642 to 1.4532 g/cm^3, respectively.

However, the density was unexpectedly reduced when the ethyl chain in $TESPAMHSO_4$ was changed to methyl of $DEMSPAMHSO_4$.

The experimental results for the 12 ILs showed that the presence of long chain alkyl or sulfonate group on the cation, of decreasing or increasing the density, is not following systematic manners. However, the density of the alkyl imidazoliums is very close to one another. These results are in agreement with recent reports of Dunstan *et al*. [267] and Ahosseini and Scurto [271].

As can see in Figure 4.10a, b and c, temperature and density show a linear correlation of more than 99.9%. Thus the linear equation can be used for calculating the density of any of the 12 ILs, at any temperature. Increasing the temperature from 20 to 80 °C did not show any significant decrease.

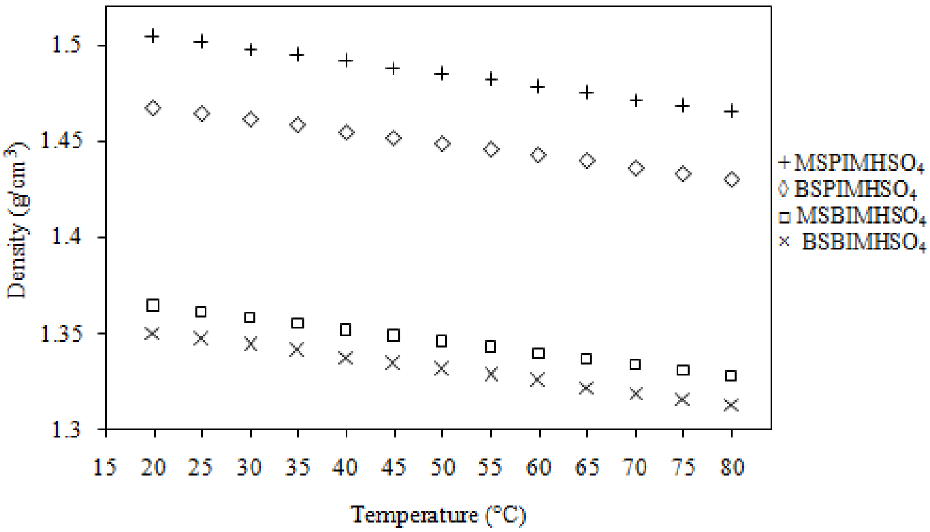

1.5
1.45
1.4
1.35
1.3
Density (g/cm 3)
15
20
25
30
35
40
45
50
55
60
65
70
75
80
Temperature (°C)
+ MSPIMHSO4
◊ BSPIMHSO4
□ MSBIMHSO4
× BSBIMHSO4

(a)

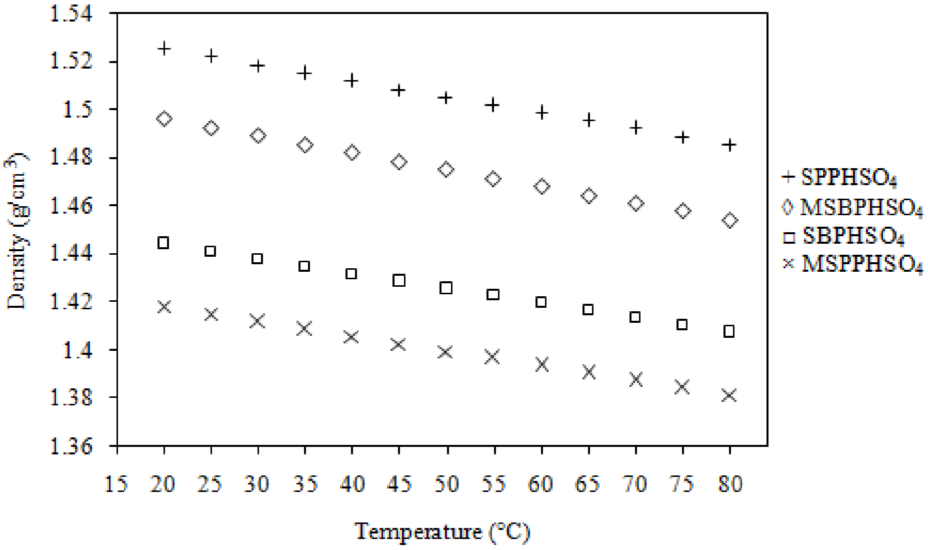

1.54
1.52
1.5
1.48
1.46
1.44
1.42
1.4
1.38
1.36
Density (g/cm 3)
15
20
25
30
35
40
45
50
55
60
65
70
75
80
Temperature (°C)
+ SPPHSO4
◊ MSBPHSO4
□ SBPHSO4
× MSPPHSO4

(b)

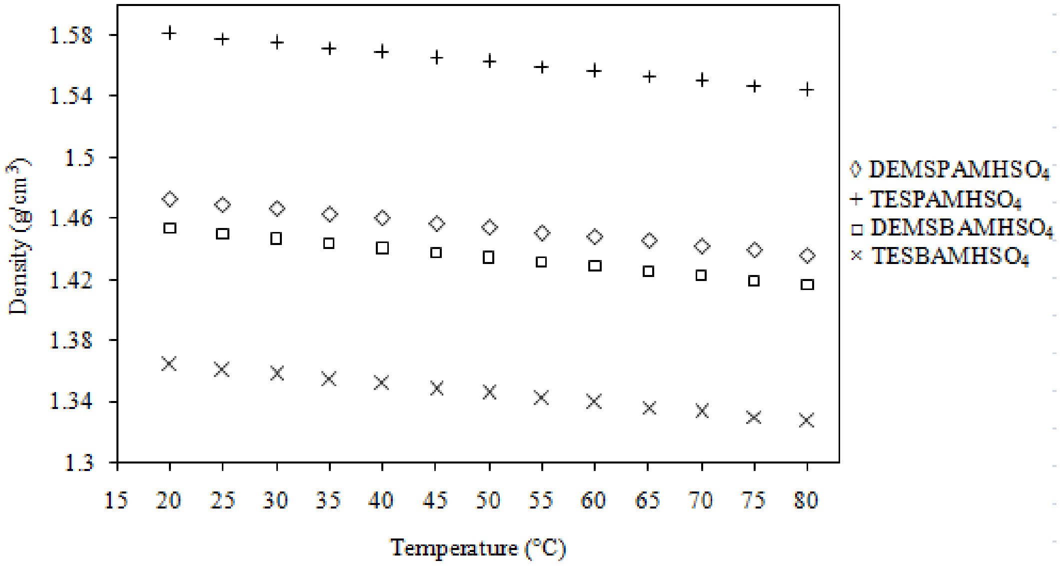

(c)

Figure 4.10 Densities as function of temperature for functionalized ILs: (a) imidazoliums, (b) pyrazoliums, and (c) ammoniums ILs.

For example as presented in Figure 4.10, $BSBIMHSO_4$ showed a small density drop from 1.3642 g/cm^3 to 1.3275 g/cm^3 when the temperature was raised from 20 to 80 °C, a reduction of only 0.0367 g/cm^3. These results indicate that temperature variation has no considerable effect on the IL densities. The same observation was made by Valderrama and Zarricueta [270] in their study on the synthesis and properties of some ILs. The density of the ILs in order of decreasing density are imidazolium > ammonium > pyrazolium.